Sensing and Bio-Sensing Research 41 (2023) 100565

Contents lists available at ScienceDirect

Sensing and Bio-Sensing Research

journal homepage: www.elsevier.com/locate/sbsr

Photonic crystal fibre for blood components sensing

Abdul Mu'iz Maidi [a,*], Md. Abul Kalam [b], Feroza Begum [a]

[a] Faculty of Integrated Technologies, Universiti Brunei Darussalam, Jalan Tungku Link, Gadong, Bandar Seri Begawan BE1410, Brunei Darussalam
[b] School of Civil and Environmental Engineering, Faculty of Engineering and Information Technology, University of Technology Sydney, NSW 2007, Australia

ARTICLE INFO

Keywords:
Blood component
Confinement loss
Photonic crystal fibre
Relative sensitivity

ABSTRACT

A photonic crystal fibre (PCF)-based sensor has been proposed and thoroughly investigated for the identification of blood components, including red blood cells, haemoglobin, white blood cells, plasma, and water. To evaluate the sensor's sensing and propagation properties, a numerical analysis was performed using the COMSOL Multiphysics software. The proposed sensor design features an octagonal core and two layers of cladding with octagonal and circular air holes. At the optimal wavelength of 7.0 μm, the extensive simulation results confirms that the proposed sensor achieves high relative sensitivity of 99.89%, 99.13%, 97.95%, 97.77%, and 96.68% for red blood cells, haemoglobin, white blood cells, plasma, and water, respectively. Furthermore, the design demonstrates favourable confinement loss, propagation constant, V-parameter, spot size, and beam divergence. Therefore, the proposed PCF-based sensor holds great promise not only for medical sensing applications but also for optical communications. Its advanced design and highly sensitive capabilities make it a valuable tool for a wide range of potential applications in the biomedical and telecommunications fields.

1. Introduction

Traditionally, optical fibres have been developed and used for telecommunication purposes. Due to technological advances, optical fibres have also been used as a tool for sensing applications, which was provided by the improving fabrication techniques. Photonic Crystal Fibres (PCFs) have unique properties such as birefringence, dispersion, and confinement loss, which can be modified by adjusting the shape and diameter of air holes and pitch [1]. PCFs are robust under harsh conditions and have numerous potential applications such as optical communication [2], imaging [3], filters [4], and sensing applications [5]. Hollow core PCFs allow for strong light-analyte interaction, leading to new sensing applications such as refractive index sensing [6], temperature sensing [7], chemical sensing [8], gas sensing [9], magnetic field measurement [10], and blood component detection [11].

Human blood is made up of different components, among which are red blood cells (RBCs), white blood cells (WBCs), haemoglobin (HB), plasma, and water. The current detection of these components are by ion chromatography [12], using gold nanoparticles [13], and piezoelectric quartz crystals [14]; for the necessary diagnostic of thalassemia, hemophilia, anemia, myeloma, and so on [15]. Hence, PCF-based biosensor has also been introduced to the application of sensing these various blood components. Singh and Kaur [16] proposed the first blood component sensor operating in the optical wavelength. The PCF follows the design of a circular ring core and four rings cladding air holes in a circular arrangement, thus, obtained relative sensitivities of 56.05%. 53.72%, 66.46%, 54.04%, and 55.09% for RBCs, WBCs, haemoglobin, plasma, and water, respectively, at their optimal wavelength. Later, the same researchers [17] enhanced the PCF sensor design by increasing the core sensing ring by 0.6 μm and all cladding air holes by about 1.5 μm. However, the relative sensitivities for the blood component analytes showed no significant change with values of 55.83%, 58.05%, 62.72%, 65.05%, and 66.47% for RBCs, haemoglobin, WBCs, plasma, and water, respectively. Islam et al. [18] have proposed a PCF-based sensor for the detection of plasma, which employs a microstructured benzene-shaped core and five layers of circular air holes in the cladding region. The performance was evaluated by analysing its relative sensitivity, confinement loss, effective area, and numerical aperture. At the optimum wavelength of 1.33 μm, the sensor achieved a high relative sensitivity of 77.84% for plasma detection. A group of researchers [19], then, introduced a porous core PCF with numerous core holes and five layers of circular cladding air holes. With emphasis on their complex design, a higher relative sensitivity results have been obtained: 80.93% for RBCs, 80.56% for WBCs, 80.13% for haemoglobin, 79.91% for plasma, and 79.39% for water. Additionally, Hossain and Podder [20] recommended a segmental PCF-based sensor for detection of blood

* Corresponding author.
E-mail addresses: 21m5101@ubd.edu.bn (A.M. Maidi), mdabul.kalam@uts.edu.au (Md.A. Kalam), feroza.begum@ubd.edu.bn (F. Begum).

https://doi.org/10.1016/j.sbsr.2023.100565
Received 15 February 2023; Received in revised form 18 April 2023; Accepted 22 May 2023
Available online 23 May 2023

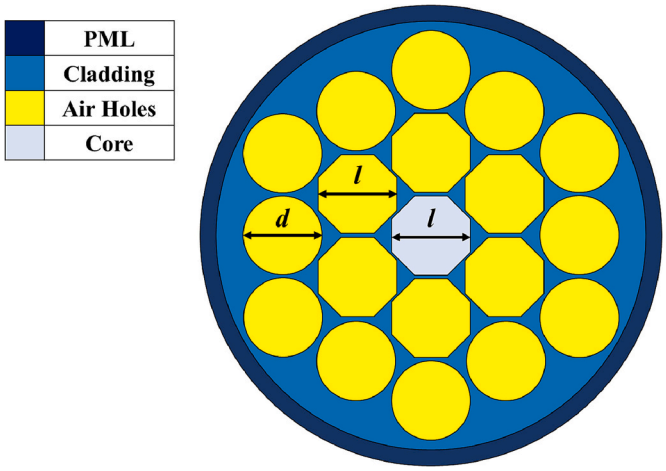

Fig. 1. Cross-sectional architecture of the proposed blood components sensor.

components. The design consists of a single rectangular core and six segments of air holes in the cladding region that enhances the relative sensitivities obtained. At the optimum parameter, the relative sensitivities are 93.50%, 92.15%, 92.41%, 90.48%, and 89.14% for RBCs, WBCs, haemoglobin, plasma, and water, respectively. Another group of researchers [21] demonstrated a high relative sensitivity for blood component sensing using a PCF. The relative sensitivities are 96.19% for RBCs, 95.57% for WBCs, 95.89% for haemoglobin, 95.39% for plasma, and 95.01% for water, respectively, through a square core and four cladding air hole segments design.

Despite the critical importance of accurate and efficient blood component detection in medical diagnosis and treatment, current sensing techniques suffer from limitations in sensitivity and specificity. This creates a significant need for the development of new, highly sensitive sensing methods that can accurately detect a range of blood components. The proposed research seeks to address this gap in knowledge by investigating the feasibility and performance of a novel PCF-based blood components sensor that offers high sensitivity. This paper presents a blood component PCF-sensor with a simpler design comprising a hollow octagonal core and two layers of cladding air holes. The proposed sensor exhibits significantly improved sensing capabilities in the optical wavelength range 2.5 μm to 7.0 μm. Numerical simulation of the design demonstrates that the proposed fibre can support excellent sensing capabilities under optimised conditions. Given that, the relative sensitivities obtained for all the blood components are above 96% and confinement losses of approximately lower than 10^{-7} dB/m about the optimum wavelength. In addition, the proposed sensor functions as a single-mode fibre by determining the V-parameter that offers beneficial results of propagation constant, spot size, and beam divergence.

This paper is organised as follows: Section 2 present the design, material used with its refractive index in the proposed PCF sensor for detecting blood components. Section 3 describes the numerical simulation methodology employed to evaluate the PCF design. Section 4 presents the results of the study, including the relative sensitivity and confinement loss of the sensor for detecting red blood cells, haemoglobin, white blood cells, plasma, and water. In addition, the implications of these results and potential applications in medical sensing and optical communications are discussed. Finally, Section 5 provides a summary of the main findings and conclusions of the study.

2. Design

The overall diameter of the proposed blood component sensor in 40.8 μm, and the cross-sectional design is shown in Fig. 1. A fully functional PCF sensor consists of core, cladding and the Perfectly Matched Layer (PML). The cladding incorporates two layers of air holes: octagonal hollow holes in the first ring and followed by circular hollow holes surrounding a single octagonal core hole. The core length l is 7.55 μm and is infiltrated with the different blood components for sensing. The octagonal cladding holes in the first ring follows the core length l = 7.55 μm and circular air hole diameter d in the second ring is 7.6 μm. The PML is set to 10% of the total diameter to consider the loss properties in the fibre and the fabrication complexity. Blood contains various components that includes water, plasma, white blood cells, haemoglobin and red blood cells with refractive indices of 1.33, 1.35, 1.36, 1.38, and 1.40, respectively [21]. The background material is fused silica and its refractive index of fused silica is determined by Sellmeier equation [22,23]:

$$n^2 = 1 + \frac{0.69617\lambda^2}{\lambda^2 - 0.0684^2} + \frac{0.40794\lambda^2}{\lambda^2 - 0.11624^2} + \frac{0.89748\lambda^2}{\lambda^2 - 9.89616^2} \quad (1)$$

where, λ is the operating wavelength.

Fabrications of PCFs has evolved throughout the years and different techniques has been introduced to ease the process of manufacture such as stacking, extrusion, 3D printing and many more [24–28]. For the fabrication of PCFs with octagonal core and cladding holes, the ultra-simplified single-step 3D printing technique is recommended, as suggested by Cordeiro et al. [29].

3. Methodology

This study employs the full vector Finite Element Method (FEM) with a Perfectly Matched Layer (PML) boundary, which is the most effective numerical approaches for engineering design simulation. This PML boundary conditions provides efficient method for evaluating the propagation properties of leaky modes in PCFs that allows evaluation in a single run.

The operating wavelength range for this study is between 2.5 and 7.0 μm, which covers the medium and long wave infrared (IR) region. To determine the results of the blood components sensor, the main measurement metric of the PCF-based sensors is the evaluation of the relative sensitivity. However, to deduce overall performance of the sensor, other optical properties are computed that includes confinement loss, chromatic dispersion, propagation constant, and V-parameter.

Relative sensitivity S represents the interaction between the light intensity and sensing analyte. [8,30,31]:

$$S = \frac{n_r}{Re(n_{\text{eff}})} \times P \quad (2)$$

where, n_r is the refractive index of the test analyte, Re(n_{eff}) is the real part of the effective refractive index, and P is the power fraction.

Power fraction P is the ratio between the power flowing through the sample in the core to the power over the total structure of the fibre. The power ratio is given by [8,31,32]:

$$P = \frac{(sample)\int Re(E_x H_y - E_y H_x)dxdy}{(total)\int Re(E_x H_y - E_y H_x)dxdy} \times 100 \quad (3)$$

where, E and H are the electric fields and magnetic fields, respectively, and the x and y subscripts represent the polarisation of these fields in x- and y-directions.

Electromagnetic waves in the waveguide of the fibre are prone to leak into the surrounding structure and confinement loss is the term for this loss of light signal. Confinement loss L is the measure of leakage of light, and it is defined as [33–35]:

$$L = \frac{40\pi}{ln(10)\lambda} Im(n_{\text{eff}}) \times 10^6 \quad (4)$$

where, Im(n_{eff}) is the imaginary part of the effective refractive index and λ is the operating wavelength.

Propagation constant β occurs for any electromagnetic signal and it is

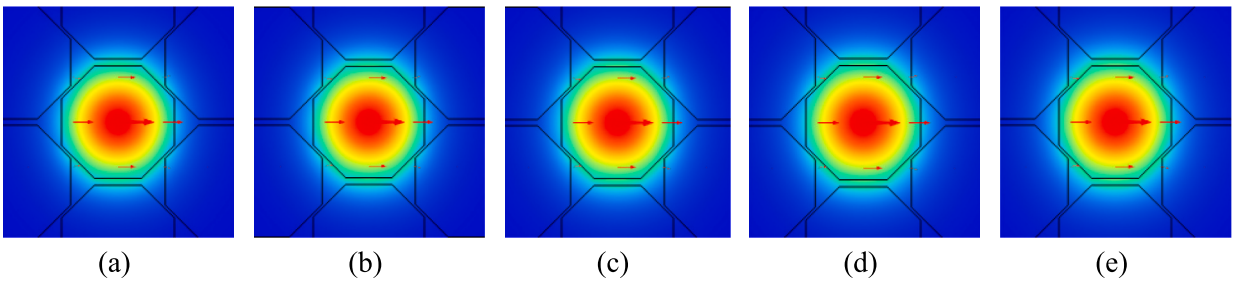

Fig. 2. Mode profile of (a) red blood cells (b) haemoglobin (c) white blood cells (d) plasma (e) water in the proposed sensor at λ = 7.0 μm. (For interpretation of the references to colour in this figure legend, the reader is referred to the web version of this article.)

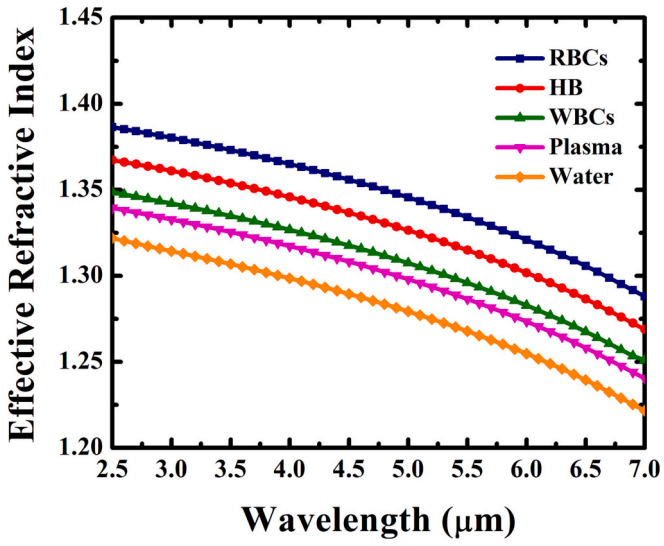

Fig. 3. Effective refractive index of the blood components sensor at different operating wavelength.

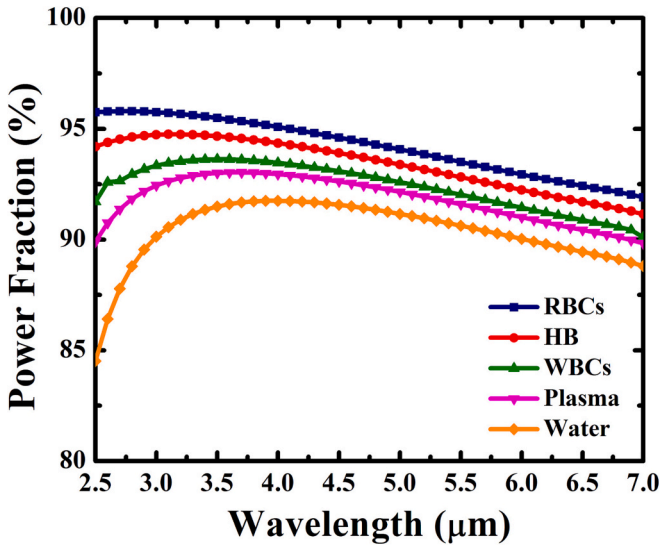

Fig. 4. Power fraction of the blood components sensor at different operating wavelength.

the variation of the amplitude spreads in a given direction [36]:

$$\beta = n_{\text{eff}}\frac{2\pi}{\lambda} \tag{5}$$

V-parameter V is the single-more propagation parameter to deduce whether the fibre is subjected to multimodal distortions, and it is defined as [37–39]:

$$V = \frac{2\pi}{\lambda}R\sqrt{n_{co}^2 - n_{cl}^2} \tag{6}$$

where, R is the radius of the core, and n_{co} and n_{cl} are the refractive index of core and cladding, respectively.

Spot size W_{eff} is the radius of the optical signal around the core of the fibre that can be determined using the Marcuse equation [40–42]:

$$W_{\text{eff}} = R \times \left(0.65 + \frac{1.619}{V^{\frac{3}{2}}} + \frac{2.879}{V^6}\right) \tag{7}$$

Beam divergence θ quantifies the light beam quality and measures the angle of spreading of light beam around the core of the fibre, which is calculated in radians by [40,41,43]:

$$\theta_{radian} = tan^{-1}\left(\frac{\lambda}{\pi W_{\text{eff}}}\right) \tag{8}$$

However, to determine the beam divergence θ in degrees, it can be found by [40,41,43]:

$$\theta_{\text{degree}} = \theta_{\text{radian}} \times \left(\frac{180}{\pi}\right) \tag{9}$$

4. Results and discussions

Several optical parameters have been considered in the analysis of the proposed PCF for the use in blood components (RBCs, HB, WBCs,

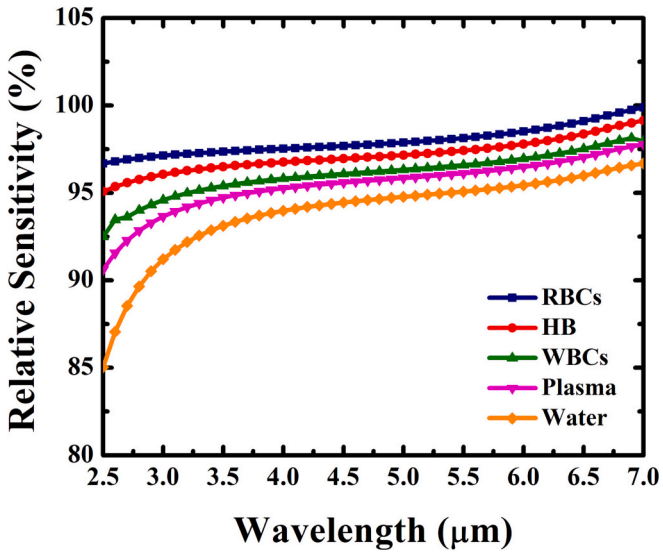

Fig. 5. Relative sensitivity of the blood components sensor at different operating wavelength.

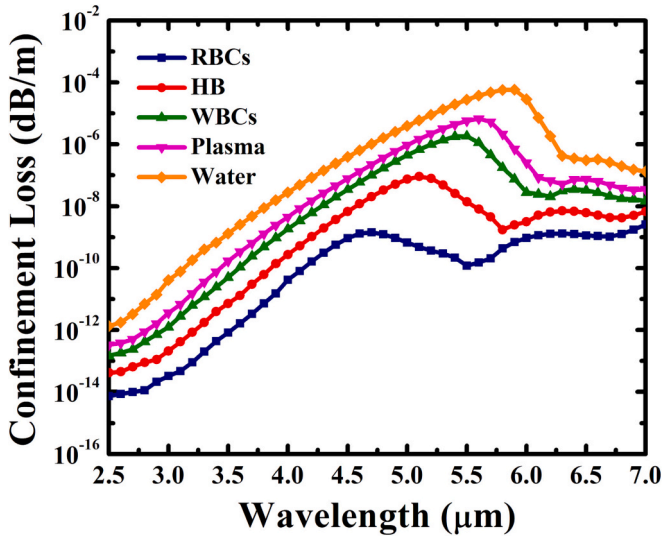

Fig. 6. Confinement loss of the blood components sensor at different operating wavelength.

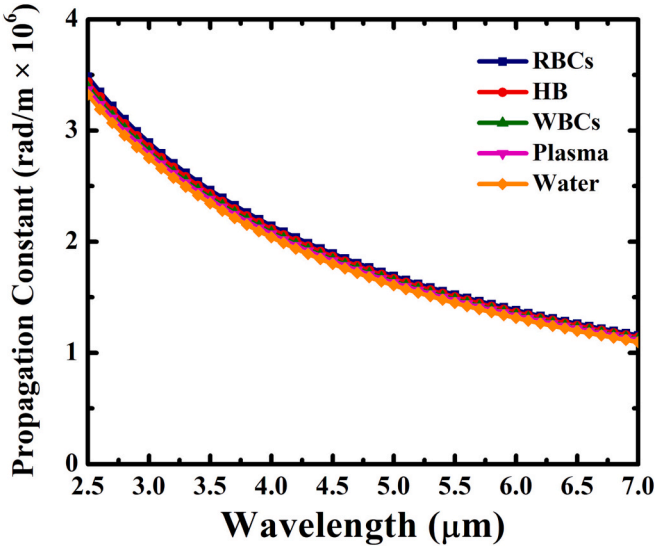

Fig. 7. Propagation constant of the blood components sensor at different operating wavelength.

plasma, and water) sensor including effective refractive index, power fraction, relative sensitivity, confinement loss, propagation constant, V-parameter, spot size, and beam divergence. Fig. 2 displays the mode distribution profile of the test analytes within the core of the fibre at operating wavelength of 7.0 μm.

Effective refractive index is obtained through the COMSOL software and the results for the test analytes are shown in Fig. 3. The effective refractive indices of these blood components rely significantly on their respective refractive index; refractive index of RBCs is the highest, followed by HB, WBCs, plasma, and water. As seen from the figure, effective refractive index of the analytes decreases as wavelength increases from 2.5 to 7.0 μm.

Power fraction results of the sensing analytes in the proposed PCF is presented in Fig. 4. The power fractions of the different blood components (RBCs, HB, WBCs, plasma, and water) follow a similar trend to one another that increases initially to a maximum percentage, respective to the analyte, and decreases consequently with the increase of operating wavelength. These results are then used to compute the relative sensitivities.

Relative sensitivity measures the interaction of optical light with the sensing analytes and the results for sensing RBCs, HB, WBCs, plasma, and water are shown in Fig. 5. Based on Eq. (2), relative sensitivity relates to the results of effective refractive index and power fraction, thus, corresponding trend is seen in the figure. In the earlier operating wavelength range, relative sensitivity of the blood components increases initially, and subsequently decreases as wavelength further increase. The obtained high relative sensitivity results are attributed to the larger dimension of the core hole. The larger size of the core hole facilitates greater infiltration of analytes into the fibre and results in enhanced light-analyte interaction, thus leading to higher relative sensitivity. The optimum wavelength of this study is defined at $\lambda = 7.0$ μm, as the highest relative sensitives are obtained at this wavelength. Therefore, at the optimum operating wavelength, the obtained relative sensitivities are 99.89% for RBC, 99.13% for HB, 97.95% for WBCs, 97.77% for plasma, and 96.68% for water.

Light signal tends to escape from the core of the fibre with respect to the wavelength, and this loss in light intensity is referred to as confinement loss. This condition aligns with the phenomenon shown in Fig. 6, which demonstrates the outcome of confinement loss of the sensing analytes in correspond to the operating wavelength. In the increasing set range of wavelength, the confinement losses increase for the blood components. Additionally, the relationship between the

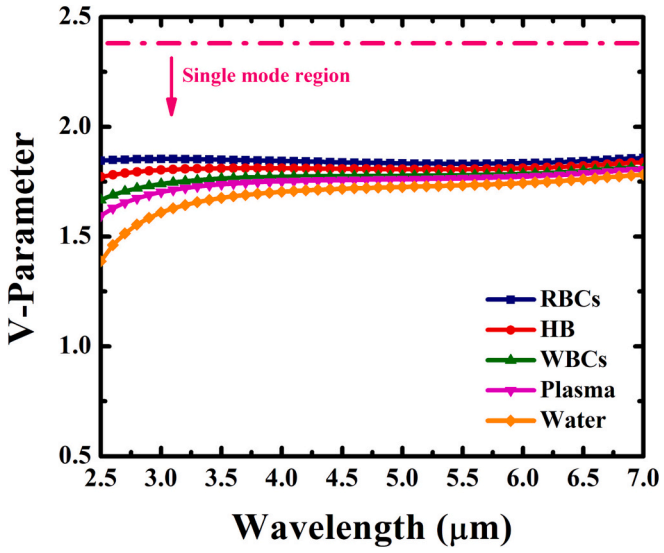

Fig. 8. V-parameter of the blood components sensor at different operating wavelength.

refractive index of the test analyte and the confinement loss can be observed, where a higher refractive index of the analytes results in lower confinement loss. This is due to the refractive index difference between the core and cladding, which leads to better light confinement in the core of the fibre. At 7.0 μm optimal wavelength, the confinement losses of 2.56×10^{-9} dB/m for RBCs, 6.74×10^{-9} dB/m for HB, 1.46×10^{-8} dB/m for WBCs, 3.51×10^{-8} dB/m for plasma, and 1.33×10^{-7} dB/m for water are dB/m, respectively.

The graphical representation of propagation constant against operating wavelength 2.5 μm to 7.0 μm is shown in Fig. 7. Propagation constant of the proposed PCF reduces gradually when the operating wavelength increases. In other words, a low propagation constant is achieved at a high wavelength. This characteristic is desirable in optical fibres, as a lower propagation constant indicates that the light signal can travel over longer distances with minimal attenuation and loss. Furthermore, this feature can also enhance the relative sensitivity of the PCF sensor, making it a preferred choice in various sensing and communication applications. Notably, the results of the different blood

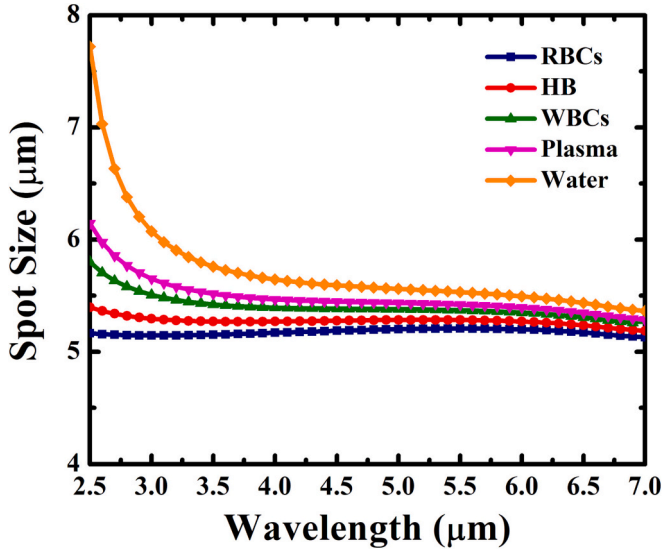

Fig. 9. Spot size of the blood components sensor at different operating wavelength.

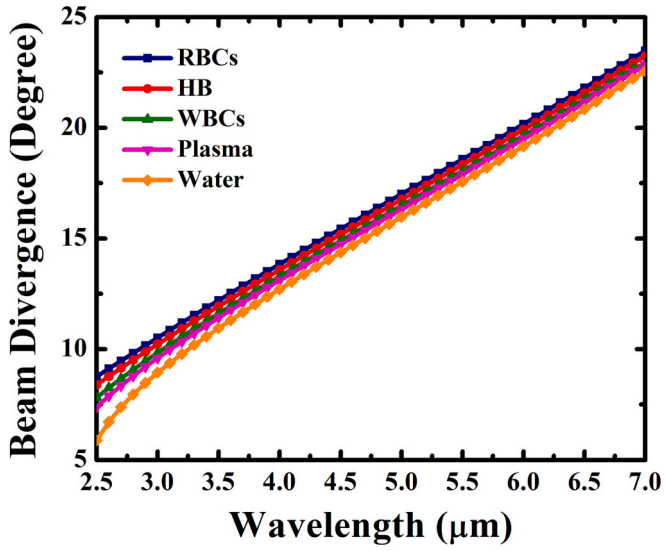

Fig. 10. Beam divergence of the blood components sensor at different operating wavelength.

components are close together, and at the operating wavelength of 7.0 μm, the propagation constants are 1.156×10^6 rad/m for RBCs, 1.139×10^6 rad/m for HB, 1.122×10^6 rad/m for WBCs, 1.113×10^6 rad/m for plasma, and 1.097×10^6 rad/m for water.

V-parameter determines whether the proposed fibre operates as a single-mode or multi-mode fibre. Fig. 8 presents the results of V-parameter for the infiltrated blood component analytes corresponding to the operating optical wavelength. The V-parameter reduces gradually as the wavelength increases; this acts in accordance to the difference of refractive index between the core and cladding decreases with increasing wavelength. V_{eff} should be less than or equal to 2.405 to deduce to be a single-mode fibre [37]. Hence, the proposed design operates as a single-mode fibre throughout the set operating wavelength.

From Eq. (7), the V-parameter can quantify the spot size. The relationship between spot size of the proposed sensor for the blood components and operating wavelength is shown in Fig. 9. Profoundly, the spot sizes of the test analytes drastically decrease at earlier wavelength and subsequently decreases gradually as the wavelength further increases. It can be seen that higher refractive index analyte produces smaller spot size. A smaller spot size is beneficial as it results in better resolution and higher sensitivity in sensing applications. This is because a smaller spot size allows for tighter focusing of the light, which can interact more extensively with the entirety of the analyte in the core. Consequently, smaller spot size can lead to more precise and accurate measurements. At optimum wavelength of 7.0 μm, the spot size for RBCs, HB, WBCs, plasma, and water are 5.13 μm, 5.19 μm, 5.28 μm, 5.29 μm, and 5.36 μm, respectively.

Referring to Eq. (8), beam divergence of the proposed PCF can be deduced from the spot size. Fig. 10 represents the beam divergence (in degrees) of each test analytes against operating wavelength, which demonstrates an increasing trend. With increasing wavelength from 2.5 to 7.0 μm, the beam divergences increase, where it profoundly follows the respective refractive indices; RBCs has the highest angle divergence and water has the smallest. All the values are less than 25°, indicating small divergence of the optical beam. This is a favourable behaviour for analyte sensing, as it implies that the light remains focused and confined over a longer distance, resulting in better sensitivity of the PCF sensor. Furthermore, a small beam divergence can also lead to improved transmission efficiency, as light can travel with less loss. The results of beam divergence in degrees are 23.48° for RBCs, 23.25° for HB, 22.88° for WBCs, 22.86° for plasma, and 22.56° for water, at wavelength $\lambda = 7.0$ μm.

Table 1 presents a detailed comparison table on important results between the proposed PCF and prior studies. In the following table, it confirms that the proposed sensor is better than the previously reported studies.

5. Conclusion

A highly sensitive, simple, photonic crystal fibre (PCF)-based blood components sensor has been developed. This sensor is capable of detecting red blood cells, haemoglobin, white blood cells, plasma, and water. The sensor design employs a two-layer cladding structure with octagonal holes in the first ring and circular holes in the second ring, along with a single octagonal core hole. The design was analysed numerically on COMSOL Multiphysics using finite element method

Table 1
Comparison table on proposed PCF against prior PCFs at optimum wavelength.

References	Design		Relative Sensitivity (%)				
	Core	Cladding	RBCs	HB	WBCs	Plasma	Water
Ref. [16]	Circular hollow ring	Circular air holes in 4 rings	56.05	66.47	53.72	54.04	55.09
Ref. [17]	Circular hollow ring	Circular air holes in 4 rings	55.83	58.05	62.72	65.05	66.47
Ref. [18]	Benzene-shaped core	Circular air holes in 5 rings	–	–	–	77.84	–
Ref. [19]	Porous core	Circular air holes in 5 rings	80.93	80.56	80.13	79.91	79.39
Ref. [20]	Rectangular hollow hole	6 hollow cladding segments	93.50	92.41	92.25	90.48	89.14
Ref. [21]	Square hollow hole	4 hollow cladding segments	96.19	95.89	95.57	95.39	95.01
Proposed PCF	Octagonal hollow hole	Octagonal and circular air holes in 2 rings	99.89	99.13	97.95	97.77	96.68

(FEM) simulation techniques.

The PCF sensor functions as a single-mode fibre and exhibits favourable results for relative sensitivity, confinement loss, propagation constant, V-parameter, spot size, and beam divergence. At the optimum wavelength of 7.0 μm, the sensor demonstrates high relative sensitivities of 99.89% for RBC, 99.13% for HB, 97.95% for WBCs, 97.77% for plasma, and 96.68% for water. These findings showcase the sensor's capabilities in detecting blood components and highlight its potential for medical sensing applications. Moreover, the sensor's favourable results for confinement loss, propagation constant, spot size, and beam divergence indicate that it may have potential applications in optical communications.

Declaration of Competing Interest

The authors declare that they have no known competing financial interests or personal relationships that could have appeared to influence the work reported in this paper.

Data availability

Data will be made available on request.

References

[1] S. Arismar Cerqueira, Recent progress and novel applications of photonic crystal fibers, Rep. Prog. Phys. 73 (2) (2010), 024401, https://doi.org/10.1088/0034-4885/73/2/024401.

[2] A. Barh, B.P. Pal, G.P. Agrawal, R.K. Varshney, B.M.A. Rahman, Specialty fibers for terahertz generation and transmission: a review, IEEE J. Sel. Top. Quantum Electron. 22 (2) (2016) 365–379, https://doi.org/10.1109/JSTQE.2015.2494537.

[3] D.M. Mittleman, Twenty years of terahertz imaging [invited], Opt. Express 26 (8) (2018) 9417, https://doi.org/10.1364/OE.26.009417.

[4] D. Chen, Stable multi-wavelength erbium-doped fiber laser based on a photonic crystal fiber Sagnac loop filter, Laser Phys. Lett. 4 (6) (2007) 437–439, https://doi.org/10.1002/lapl.200710003.

[5] X. Wang, O.S. Wolfbeis, Fiber-optic chemical sensors and biosensors (2015–2019), Anal. Chem. 92 (1) (2020) 397–430, https://doi.org/10.1021/acs.analchem.9b04708.

[6] N. Luan, J. Yao, A hollow-core photonic crystal fiber-based SPR sensor with large detection range, IEEE Photon. J. 9 (3) (2017) 1–7, https://doi.org/10.1109/JPHOT.2017.2694479.

[7] R. Zeltner, R. Pennetta, S. Xie, P.S.J. Russell, Flying particle microlaser and temperature sensor in hollow-Core photonic crystal Fiber, Opt. Lett. 43 (7) (2018) 1479, https://doi.org/10.1364/OL.43.001479.

[8] M.E. Rahaman, R.H. Jibon, H.S. Mondal, M.B. Hossain, A.A.-M. Bulbul, R. Saha, Design and optimization of a PCF-based chemical sensor in THz regime, Sens. Bio-Sens. Res. 32 (2021), 100422, https://doi.org/10.1016/j.sbsr.2021.100422.

[9] A. Abbaszadeh, S. Makouei, S. Meshgini, New hybrid photonic crystal fiber gas sensor with high sensitivity for ammonia gas detection, Can. J. Phys. 100 (2) (2022) 129–137, https://doi.org/10.1139/cjp-2021-0016.

[10] Y. Zhao, R. Lv, Y. Ying, Q. Wang, Hollow-core photonic crystal fiber fabry–perot sensor for magnetic field measurement based on magnetic fluid, Opt. Laser Technol. 44 (4) (2012) 899–902, https://doi.org/10.1016/j.optlastec.2011.11.011.

[11] M.M.A. Eid, M.A. Habib, M.S. Anower, A.N.Z. Rashed, Hollow core photonic crystal fiber (PCF)–based optical sensor for blood component detection in terahertz Spectrum, Braz. J. Phys. 51 (4) (2021) 1017–1025, https://doi.org/10.1007/s13538-021-00906-7.

[12] E. Jaszczak, M. Ruman, S. Narkowicz, J. Namieśnik, Ż. Polkowska, Development of an analytical protocol for determination of cyanide in human biological samples based on application of ion chromatography with pulsed amperometric detection, J. Anal. Methods Chem. 2017 (2017) 1–7, https://doi.org/10.1155/2017/7157953.

[13] L. Liu, X. Wang, J. Yang, Y. Bai, Colorimetric sensing of selenocystine using gold nanoparticles, Anal. Biochem. 535 (2017) 19–24, https://doi.org/10.1016/j.ab.2017.07.020.

[14] Y.G. Timofeyenko, J.J. Rosentreter, S. Mayo, Piezoelectric quartz crystal microbalance sensor for trace aqueous cyanide ion determination, Anal. Chem. 79 (1) (2007) 251–255, https://doi.org/10.1021/ac060890m.

[15] P. Sharma, P. Sharan, Design of Photonic Crystal Based Ring Resonator for detection of different blood constituents, Opt. Commun. 348 (2015) 19–23, https://doi.org/10.1016/j.optcom.2015.03.015.

[16] S. Singh, V. Kaur, Photonic crystal fiber sensor based on sensing ring for different blood components: Design and analysis, in: 2017 Ninth International Conference on Ubiquitous and Future Networks (ICUFN), IEEE, 2017, pp. 399–403, https://doi.org/10.1109/ICUFN.2017.7993816.

[17] V. Kaur, S. Singh, Design approach of solid-core photonic crystal fiber sensor with sensing ring for blood component detection, J. Nanophoton. 13 (02) (2019) 1, https://doi.org/10.1117/1.JNP.13.026011.

[18] M.T. Islam, M.G. Moctader, K. Ahmed, S. Chowdhury, Benzene shape photonic crystal fiber based plasma sensor: design and analysis, Photon. Sensors 8 (3) (2018) 263–269, https://doi.org/10.1007/s13320-018-0495-8.

[19] K. Ahmed, F. Ahmed, S. Roy, B.K. Paul, M.N. Aktar, D. Vigneswaran, M.S. Islam, Refractive index-based blood components sensing in terahertz spectrum, IEEE Sensors J. 19 (9) (2019) 3368–3375, https://doi.org/10.1109/JSEN.2019.2895166.

[20] M.B. Hossain, E. Podder, Design and investigation of PCF-based blood components sensor in terahertz regime, Appl. Phys. A Mater. Sci. Process. 125 (12) (2019) 861, https://doi.org/10.1007/s00339-019-3164-x.

[21] A.A.-M. Bulbul, R.H. Jibon, S. Biswas, S.T. Pasha, M.A. Sayeed, Photonic crystal fiber-based blood components detection in THz regime: design and simulation, Sensors Int. 2 (2021), 100081, https://doi.org/10.1016/j.sintl.2021.100081.

[22] M.A. Habib, M.S. Anower, A. AlGhamdi, O.S. Faragallah, M.M.A. Eid, A.N. Z. Rashed, Efficient way for detection of alcohols using hollow core photonic crystal fiber sensor, Opt. Rev. 28 (4) (2021) 383–392, https://doi.org/10.1007/s10043-021-00672-6.

[23] M.A. Habib, L.F. Abdulrazak, M. Magam, L. Jamal, K.K. Qureshi, Design of a highly sensitive photonic crystal fiber sensor for sulfuric acid detection, Micromachines 13 (5) (2022) 670, https://doi.org/10.3390/mi13050670.

[24] A. Ghazanfari, W. Li, M.C. Leu, G.E. Hilmas, A novel freeform extrusion fabrication process for producing solid ceramic components with uniform layered radiation drying, Addit. Manuf. 15 (2017) 102–112, https://doi.org/10.1016/j.addma.2017.04.001.

[25] H. Ebendorff-Heidepriem, J. Schuppich, A. Dowler, L. Lima-Marques, T.M. Monro, 3D-printed extrusion dies: a versatile approach to optical material processing, Opt. Mater. Express 4 (8) (2014) 1494, https://doi.org/10.1364/OME.4.001494.

[26] W. Talataisong, R. Ismaeel, S.R. Sandoghchi, T. Rutirawut, G. Topley, M. Beresna, G. Brambilla, Novel method for manufacturing optical fiber: extrusion and drawing of microstructured polymer optical fibers from a 3D printer, Opt. Express 26 (24) (2018) 32007, https://doi.org/10.1364/OE.26.032007.

[27] Z. Liu, C. Wu, M.-L.V. Tse, H.-Y. Tam, Fabrication, characterization, and sensing applications of a high-birefringence suspended-core fiber, J. Lightwave Technol. 32 (11) (2014) 2113–2122, https://doi.org/10.1109/JLT.2014.2319818.

[28] S. Atakaramians, V.S. Afshar, H. Ebendorff-Heidepriem, M. Nagel, B.M. Fischer, D. Abbott, T.M. Monro, THz porous fibers: design, fabrication and experimental characterization, Opt. Express 17 (16) (2009) 14053, https://doi.org/10.1364/OE.17.014053.

[29] C.M.B. Cordeiro, A.K.L. Ng, H. Ebendorff-Heidepriem, Ultra-simplified single-step fabrication of microstructured optical fiber, Sci. Rep. 10 (1) (2020) 9678, https://doi.org/10.1038/s41598-020-66632-3.

[30] A.M. Maidi, I. Yakasai, P.E. Abas, M.M. Nauman, R.A. Apong, S. Kaijage, F. Begum, Design and simulation of photonic crystal fiber for liquid sensing, Photonics 8 (1) (2021) 16, https://doi.org/10.3390/photonics8010016.

[31] M.M. Hasan, T. Pandey, M.A. Habib, Highly sensitive hollow-core fiber for spectroscopic sensing applications, Sens. Bio-Sens. Res. 34 (2021), 100456, https://doi.org/10.1016/j.sbsr.2021.100456.

[32] A.M. Maidi, P.E. Abas, P.I. Petra, S. Kaijage, N. Zou, F. Begum, Theoretical considerations of photonic crystal fiber with all uniform-sized air holes for liquid sensing, Photonics 8 (7) (2021) 249, https://doi.org/10.3390/photonics8070249.

[33] A.M. Maidi, N. Shamsuddin, W.-R. Wong, S. Kaijage, F. Begum, Characteristics of ultrasensitive hexagonal-cored photonic crystal fiber for hazardous chemical sensing, Photonics 9 (1) (2022) 38, https://doi.org/10.3390/photonics9010038.

[34] E. Podder, R.H. Jibon, M.B. Hossain, A. Al-Mamun Bulbul, S. Biswas, M.A. Kabir, Alcohol sensing through photonic crystal fiber at different temperature, Opt. Photon. J. 08 (10) (2018) 309–316, https://doi.org/10.4236/opj.2018.810026.

[35] A.A.-M. Bulbul, F. Imam, M.A. Awal, M.A.P. Mahmud, A novel ultra-low loss rectangle-based porous-core PCF for efficient THz waveguidance: design and numerical analysis, Sensors 20 (22) (2020) 6500, https://doi.org/10.3390/s20226500.

[36] K.R. Priya, A.S. Raja, D.S. Sundar, Design of a dual-core liquid-filled photonic crystal fiber coupler and analysis of its optical characteristics, J. Opt. Technol. 83 (9) (2016) 569, https://doi.org/10.1364/JOT.83.000569.

[37] F. Zhang, M. Zhang, X. Liu, P. Ye, Design of wideband single-polarization single-mode photonic crystal fiber, J. Lightwave Technol. 25 (5) (2007) 1184–1189, https://doi.org/10.1109/JLT.2007.893031.

[38] A. Habib, S. Anower, I. Haque, Highly sensitive hollow core spiral fiber for chemical spectroscopic applications, Sensors Int. 1 (2020), 100011, https://doi.org/10.1016/j.sintl.2020.100011.

[39] S. Rana, M. Saiful Islam, M. Faisal, K.C. Roy, R. Islam, S.F. Kaijage, Single-mode porous fiber for low-loss polarization maintaining terahertz transmission, Opt. Eng. 55 (7) (2016), 076114, https://doi.org/10.1117/1.OE.55.7.076114.

[40] D. Paul, R. Biswas, N.S. Bhattacharyya, Investigating photonic crystal fiber within E to L communication band with different material composites, Optik (Stuttg) 126 (23) (2015) 4640–4645, https://doi.org/10.1016/j.ijleo.2015.08.075.

[41] M.S. Islam, B.K. Paul, K. Ahmed, S. Asaduzzaman, M.I. Islam, S. Chowdhury, S. Sen, A.N. Bahar, Liquid-infiltrated photonic crystal fiber for sensing purpose:

design and analysis, Alex. Eng. J. 57 (3) (2018) 1459–1466, https://doi.org/10.1016/j.aej.2017.03.015.

[42] F.A. Mou, M.M. Rahman, M.R. Islam, M.I.H. Bhuiyan, Development of a photonic crystal fiber for THz wave guidance and environmental pollutants detection, Sens. Bio-Sens. Res. 29 (2020), 100346, https://doi.org/10.1016/j.sbsr.2020.100346.

[43] M.R. Islam, A.N.M. Iftekher, F.A. Mou, M.M. Rahman, M.I.H. Bhuiyan, Design of a topas-based ultrahigh-sensitive PCF biosensor for blood component detection, Appl. Phys. A Mater. Sci. Process. 127 (2) (2021) 109, https://doi.org/10.1007/s00339-020-04261-3.